Food Chemistry: X 22 (2024) 101273

Contents lists available at ScienceDirect

Food Chemistry: X

journal homepage: www.sciencedirect.com/journal/food-chemistry-x

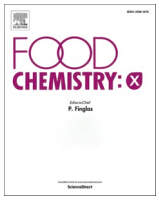

Reverse design of haptens based on antigen spatial conformation to prepare anti-capsaicinoids&gingerols antibodies for monitoring of gutter cooking oil

Kunying Nie [a,c,d,1], Jiali Zhang [a,c,d,1], Haitao Xu [a,c,d], Keyun Ren [a,c,d], Chunlei Yu [a,c,d], Qi Zhang [b,e,f], Falan Li [a,c,d], Qingqing Yang [a,c,d,*]

[a] School of Agricultural Engineering and Food Science, Shandong University of Technology, No. 266 Xincun Xilu, Zibo 255049, Shandong Province, China
[b] Oil Crops Research Institute of the Chinese Academy of Agricultural Sciences, Wuhan 430062, China
[c] Shandong Provincial Engineering Research Center of Vegetable Safety and Quality Traceability, No. 266 Xincun Xilu, Zibo 255049, Shandong Province, China
[d] Zibo City Key Laboratory of Agricultural Product Safety Traceability, No. 266 Xincun Xilu, Zibo 255049, Shandong Province, China
[e] Key Laboratory of Detection for Mycotoxins, Ministry of Agriculture and Rural Affairs, Wuhan 430062, China
[f] Laboratory of Risk Assessment for Oil-seeds Products, Wuhan, Ministry of Agriculture and Rural Affairs, Wuhan 430062, China

ARTICLE INFO

Keywords:
Gutter cooking oil
Broad-spectrum monoclonal antibodies
Molecular docking
Virtual screening

ABSTRACT

Rapid simultaneous detection of multi-component adulteration markers can improve the accuracy of identification of gutter cooking oil in edible oil, which is made possible by broad-spectrum antibody (bs-mAb). This study used capsaicinoids (CPCs) and gingerol derivatives (GDs) as adulteration markers, and two broad-spectrum haptens (bs-haptens) were designed and synthesized based on a reverse design strategy of molecular docking. Electrostatic potential (ESP) and monoclonal antibodies (mAbs) preparation verified the strategy's feasibility. To further investigate the recognition mechanism, five other reported antigens and mAbs were also used. Finally, the optimal combination (Hapten 5-OVA/1-F12) and key functional groups (f-groups) were determined. The half maximal inhibitory concentration (IC_{50}) for CPCs-GDs was between 88.13 and 499.16 ng/mL. Meanwhile, a preliminary lateral flow immunoassay (LFIA) study made practical monitoring possible. The study provided a theoretical basis for the virtual screening of bs-haptens and simultaneous immunoassay of multiple exogenous markers to monitor gutter oil rapidly and accurately.

1. Introduction

As an essential source of nutrients for regular metabolism, edible oil plays an important role in infant growth and disease prevention (Chapa-Oliver & Mejía-Teniente, 2016). In addition, the unique physical properties of edible oils are indispensable in diet and cuisine. However, some illegal businesses add gutter cooking oil into edible oils for the purpose of being sold, driven by their own interests (Tan et al., 2017). This has resulted in frequent occurrences of cooking oil safety problems. (Rifna et al., 2022; Visciano & Schirone, 2021). Refined gutter cooking oil which is complex to detect, has been one of the most concerning problems of current food quality control in developing countries (Wang et al., 2019; Yang et al., 2022). It is a difficult problem and challenge that threatens the healthy development of human beings, social harmony and stability (Wang, Gao, Xing, & Xiong, 2020; Ye & Meng, 2022). According to many relevant literatures, routine detection should be combined with a number of indicators as the basis to judge whether the oil sample is adulterated, such as cholesterol, electrical conductivity, acid value, iodine value, etc. (Tan et al., 2017; Wang et al., 2020; Wu et al., 2021). Although these indicators can improve the identification efficiency, different indicators require different sample pretreatment and skilled technicians (Amirav, Neumark, Margolin Eren, Fialkov, & Tal, 2021; Tan et al., 2017; Yang et al., 2021). Therefore, we believe that overcoming the problems such as time-consuming, complicated operations and single index is an effective way to realize the rapid detection of refined gutter cooking oil (Huang et al., 2021).

* Corresponding author at: School of Agricultural Engineering and Food Science, Shandong University of Technology, No. 266 Xincun Xilu, Zibo 255049, Shandong Province, China
E-mail address: yqqing@sdut.edu.cn (Q. Yang).
[1] These authors contributed to the work equllly and should be regarded as co-first authors.

https://doi.org/10.1016/j.fochx.2024.101273
Received 22 November 2023; Received in revised form 24 February 2024; Accepted 6 March 2024
Available online 11 March 2024

As a widely used detection method, immunoassay has been widely used in food, environment, medicine, and other detection fields (Li et al., 2021). Antibody, as a recognition element, plays a vital role in immunoassay. The bs-mAb, which recognizes a group of compounds with similar chemical structures, provides an economical way to detect multiple contaminants (Xu et al., 2009; Zou et al., 2022). This provides an effective way to solve the problem of the single index of gutter cooking oil. However, the structural design of immune hapten is the prerequisite for generating bs-mAb (Chen et al., 2021; Zeng et al., 2021). The design of bs-hapten and the selection of analyte are the keys to achieving multi-index detection. How to effectively screen hapten and improve the efficiency of antibody preparation needs our thinking and exploration.

With the effect of improving appetite and promoting digestion, capsaicinoids (CPCs, shown in Table 1), mainly including Capsaicin (CPC), N-vanillylnonanamide (N—V), dihydrocapsaicin (DCPC), and gingerol derivatives (GDs), including 6-gingerol (6-GG), 6-shogaol (6-SG), vanillylacetone (VLT), are widely popular condiments (Aziz et al., 2020; Crapnell & Banks, 2021; Dalsasso, Valencia, & Monteiro, 2022; Shen et al., 2020). The characteristic of stable physicochemical properties (Bai et al., 2021; Wu et al., 2021; Zhang et al., 2022; Zhang et al., 2022) and fat-soluble makes it challenging to separate from oils. Many studies have shown the feasibility of CPCs as markers for the adulteration of gutter cooking oil (Ma et al., 2016; Wu et al., 2022; Yang et al., 2016). Such as a study found that CPCs are not detected in most edible oils, and the background value of CPCs in peanut oil spans from 0 to 1.8 μg/kg (Guo, Li, Gao, Zhang, & Li, 2016). Some research institutions also use the total CPCs content of 1.0 μg/kg as the limit (Zhang, Ma, et al., 2022, Zhang, Zhang, et al., 2022). GDs are composed of multiple mixtures. Numerous studies have shown that 6-GG is the highest primary active ingredient in gingerols, which provides a new option for labeling exogenous adulteration in gutter cooking oil (Dalsasso et al., 2022; Promdam, Khuituan, & Panichayupakaranant, 2022). However, the chemical properties of 6-GG are unstable, the active hydrogen of C4 in the molecular structure is easily dehydrated with the C5 hydroxyl group to form 6-SG. Under heating and alkaline conditions, the C4 and C5 of 6-GG would be broken to form VLT and the corresponding aldehyde (Bhattarai, Tran, & Duke, 2001). The mutual conversion of 6-GG and 6-SG exists in the conventional processing of gutter cooking oil. There are bottlenecks in the determination of acid value by traditional methods, especially in the process of dehydration and the addition of antioxidants (Lu & Wu, 2014; Xu, Xu, Xiong, Chen, & Li, 2014) Therefore, 6-GG, 6-SG, and VLT are the representative components of GDs in gutter cooking oil. The development of bs-mAb to CPCs-GDs has become an effective method to solve the problem of a single index, which can significantly improve the reliability of detection and discrimination results.

The antigen-antibody recognition mechanism is the basis of immunoassay (Ceballos-Alcantarilla, Abad-Fuentes, Agulló, Abad-Somovilla, & Mercader, 2021). Understanding the recognition mechanism of bs-mAb has important theoretical significance and practical value for the designing of bs-hapten, the screening of high-quality monoclonal antibodies (mAbs), the application performance of mAbs and the establishment of immunoassay methods (Sun et al., 2022). Computational modeling technologies, which have the advantages of less-laborious, high-throughput, non-reagent consuming and cost-effective (Zou et al., 2022), are powerful tools to illustrate the interaction between ligands and receptors. For example, homology modeling and molecular docking

Table 1
Specific evaluation of mAbs to CPCs and GDs.

Chemicals		1-F12		1-G12		1-D6	
		IC_{50} (ng/mL)	CR (%)	IC_{50} (ng/mL)	CR (%)	IC_{50} (ng/mL)	CR (%)
6-GG	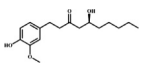	506.23	100.00	560.59	100.00	59.17	100.00
6-SG	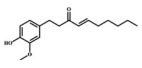	974.99	51.92	1847.86	30.31	657.56	9.00
VLT		680.32	74.41	1020.39	54.94	165.14	35.83
CPC	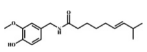	584.43	86.62	1229.06	45.61	>4000	<1.48
DCPC	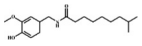	557.14	90.86	700.85	79.99	969.82	6.10
N-V	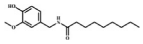	251.58	201.22	383.16	146.31	2126.35	2.78
Ferulic acid		>4000	<12.66	>4000	<14.01	1927.36	3.07
IsoFerulic acid		>4000	<12.66	>4000	<14.01	2128.07	2.78
Vanillin		>4000	<12.66	>4000	<14.01	1981.61	2.99
Trans-Ferulic acid		>4000	<12.66	>4000	<14.01	>4000	<1.48
Vanillic acid		>4000	<12.66	>4000	<14.01	1717.20	3.45
2-2-Hydroxy-3-methoxy-5-(3-oxodecyl) benzoic acid	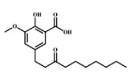	>4000	<12.66	>4000	<14.01	1952.80	3.03
2-Cyano-N-(3-methoxybenzyl) acetamide	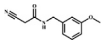	>4000	<12.66	>4000	<14.01	>4000	<1.48
3-(4-Hydroxy-3-methoxyphenyl) propionic Acid	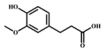	>4000	<12.66	>4000	<14.01	2175.33	2.72

play an important role in exploring molecular mechanisms and are widely used in drug screening (Abdu-Allah, Wu, Lin, & Tseng, 2020; Najar-Ahmadi et al., 2021), immunoassay (Bai et al., 2021; Zou et al., 2022), food research and other fields (Javaheri-Ghezeldizaj, Mahmoudpour, Yekta, & Dolatabadi, 2020) Our previous study on the mechanism of CPCs antigen-antibody recognition have effectively guided the establishment of electrochemical immunoassay, which further improve the sensitivity, specificity and stability of immunosensors (Sun et al., 2022). In addition, to explore the unity of computer-aided engineering and practical, it is necessary to study the key functional groups (f-groups) from the experimental level. The research on the multi-specific recognition mechanism of mAbs is significant for designing haptens and establishing of immunoassay methods. Using the existing mAbs to speed up the screening of bs-haptens and the acquisition of mAbs is meaningful and interesting.

In this study, two bs-haptens of CPCs-GDs were reverse designed and synthesized based on molecular docking results between CPCs-mAb D8 (5-D8) and CPCs-GDs. ESP analysis of haptens and its conjugates with tripeptide containing lysine fragment (Asp-Lys-His) from BSA provided a theoretical support for the feasibility of the novel hapten design strategy. Finally, three cell lines that could produce mAbs to CPCs-GDs were eventually obtained, verifying the feasibility of our hapten design. At the same time, five collected complete antigens and their corresponding mAbs were combined to cross with ours to clarify the recognition mechanism further. It provided the theoretical basis and technical support for the simultaneous immunoassay of various small molecule exogenous markers in edible oil, verified by lateral flow immunoassay (LFIA). The final combination had an excellent recognition of CPCs-GDs, and IC_{50} was from 88.13 ng/mL to 499.16 ng/mL.

2. Materials and methods

2.1. Reagents and apparatus

CPC, DCPC, N—V, 6-SG, 6-GG, VLT, ferulic acid, trans-ferulic acid, isoferulic acid, vanillic acid, vanillin, N-(1,3-Benzodioxol-5-ylmethyl)-2-cyanoacetamide, 2-cyano-N-(3-methoxyphenyl) ethanamide urea hydrogen peroxide, 3,3′,5,5′-tetramethylbenzidine (TMB) were purchased from Aladdin Co., Ltd. (Shanghai, China). Capsaicin complete antigen (Hapten 2-BSA/OVA) and antibody (2-LD2), Dihydrocapsaicin complete antigen (Hapten 3-BSA/OVA) and antibody (3-LD3) purchased from Shandong Lvdu Biotechnology Co., Ltd. (Shandong, China). (*E*)-N-(4-hydroxy-3-methoxybenzyl)-4-oxopent-2-enamide complete antigen (Hapten 4-BSA/OVA) and antibody (4-AT4) Anti-Biotechnology Co., Ltd. (Shenzhen, China). N-(4-hydroxy-3-methoxybenzyl)-4-oxopentanamide complete antigen (Hapten 5-BSA/OVA) and antibodies (5-3H1 and 5-D8) purchased from Oil Crops Research Institute, Chinese Academy of Agricultural Sciences (Wuhan, China). Ferulic acid complete antigen (Hapten 6-BSA/OVA) and antibody (6-AT6) were purchased from Anti-Biotechnology Co., Ltd. (Shenzhen, China). Pyrrolidine, ethylic acid, 2-Hydroxy-3-Methoxy benzoic acid, trifluoroacetic acid (TFA), and hexamethylenetetramine were bought from Alta Scientific Co., Ltd. (Tianjin, China). 2-hydroxy-3-methoxy-5-(3-oxodecyl) benzoic acid, bovine serum albumin (BSA), ovalbumin (OVA), dicyclohexylcarbodiimide (DCC), N-hydroxysuccinimide (NHS), *N*, *N*-dimethylformamide (DMF), hypoxanthine/thymidine/aminopterin (HAT), hypoxanthine/thymidine (HT), incomplete Freund's adjuvant (IFA), complete Freund's adjuvant (CFA), PEG 1450, were from Sigma-Aldrich (St. Louis, MO, USA). Cell culture medium (DMEM) was acquired from HyClone (Cytiva, USA). Fetal calf serum was obtained from Zhejiang Tianhang Biotechnology Co., Ltd. (Zhejiang, China). Goat anti-mouse IgG conjugated to horseradish peroxidase (GAM-HRP) and carboxyl-functionalized ZnCdSe/ZnS quantum dots (QDs) (emission maximum at 525 nm) was purchased from Shandong Lvdu Biotechnology Co., Ltd. (Shandong China). Rabbit anti-sheep IgG was bought from Beijing Biodragon Immunotechnologies Co., Ltd. All components of the LFIA, including plastic adhesive backing, nitrocellulose membrane NC 90, sample pad, and absorbent pad for the assembly of LFIA, was obtained from the Shanghai Jenin Biotechnology Co., Ltd. (Shanghai, China).

The commonly used buffer solutions in the laboratory mainly include Coating buffer (0.5 mol L^{-1} carbonate buffer, pH 9.6); Phosphate buffer solution (PBS buffer, 0.01 mol L^{-1}, pH 7.4); Blocking buffer (5% skim milk powder (*w/v*)); Washing buffer (PBST, PBS buffer with 0.05% Tween-20 (*v*/v), pH 7.4); Stopping reagent (2 mol L^{-1} H_2SO_4). Capsaicin, Dihydrocapsaicin, and N-vanillylnonanamide, 6-Gingerol, 6-Shogaol, Vanillylacetone standard storage solution (1 mg/mL) were prepared with 70% methanol water, respectively. They were stored at 4 °*C*. *ELISA* (including capsaicin, dihydrocapsaicin, N-vanillylnonanamide, 6-Gingerol, 6-Shogaol, and Vanillylacetone) were prepared by diluting the stock solutions with 10% methanol-PBS in a ratio of 1:1:1:1:1:1. In the case of uncertainty in the ratio of the presence of capsaicinoids and gingerol derivatives, the 1:1:1:1:1:1:1:1:1 ratio was chosen in this study to simulate the actual samples for the experiments.

Polystyrene microtiter plates and 96-well cell culture plates were purchased from Corning Incorporated (Costar 3590 and 3599, Corning, NY). Nuclear magnetic resonance (NMR) spectrometry DRX-400 (Bruker, Rheinstetten, Germany) and the liquid chromatography-mass spectrometer (LC-MS) (Orbitrap LTQ XL, Thermo Fisher Scientific, USA) were used to confirm the hapten structures.

2.2. Homology modeling and molecular docking

The software Molecular Operating Environment v2018.01 (MOE; Chemical Computing Group Inc., Montreal, Canada) was used to construct homology-based models of antibody structures. Amber10: EHT force field was implemented in MOE. The Fv region was built by searching for appropriate template frameworks (FR) in the built-in antibody database. Up to 125 intermediate models were built for further scoring. GB/VI solvation was used for ranking the intermediate models. The best GB/VI score model was chosen for final energy minimization.

The 2D structures of 6-GG and VLT were prepared by molecule and protein build module in MOE and converted to 3D structure through energy minimization. The optimized antibody was chosen as a receptor by homology modeling. The docking workflow followed the "induced fit" protocol, in which the side chains of the receptor binding site were allowed to move according to ligand conformations, with a constraint on their positions. For the ligand, all docked poses were ranked by London dG scoring first, then a force field refinement was carried out on the top 30 poses, followed by a rescoring of GBVI/WSA dG. The final best-ranked pose was selected.

2.3. Optimization of geometric conformation and ESP analysis of Haptens

Gaussian software (G16 C.01, Gaussian Inc., USA) and GaussView 6 (GV6.1.1, Gaussian Inc., USA) were used to quantitatively calculate the lowest energy conformation and ESP of Hapten 1–7 (Zhang, Ma, et al., 2022). In addition, based on ESP analysis, a tripeptide containing a lysine fragment (Asp-Lys-His) trapped from BSA was conjugated with hapten. To some extent, it reflected the relationship between hapten structure and the spatial conformation and electrostatic potential changes of artificial antigens.

2.4. Synthesis of Haptens and Hapten-Protein (hapten-Pr) conjugates

A synthetic pathway of Hapten 1 (6-(4-hydroxy-3-methoxyphenyl)-4-oxohexanoic acid.) and Hapten 7 (2-hydroxy-3-methoxy-5-(3-oxodecyl) benzoic acid.) were shown in Fig. S1. Hapten 1: as shown in Fig. 1, Compound 1–1 (1.16 g, 0.01 mol), tetrahydropyrrole (0.071 g, 0.001 mol) and AcOH (0.06 g, 0.001 mol) were dissolved in 10 mL toluene. Compound 1–2 (1.52 g, 0.01 mol), which dissolved in 26 mL methylbenzene was added dropwise when the temperature rises to 40 °C, and

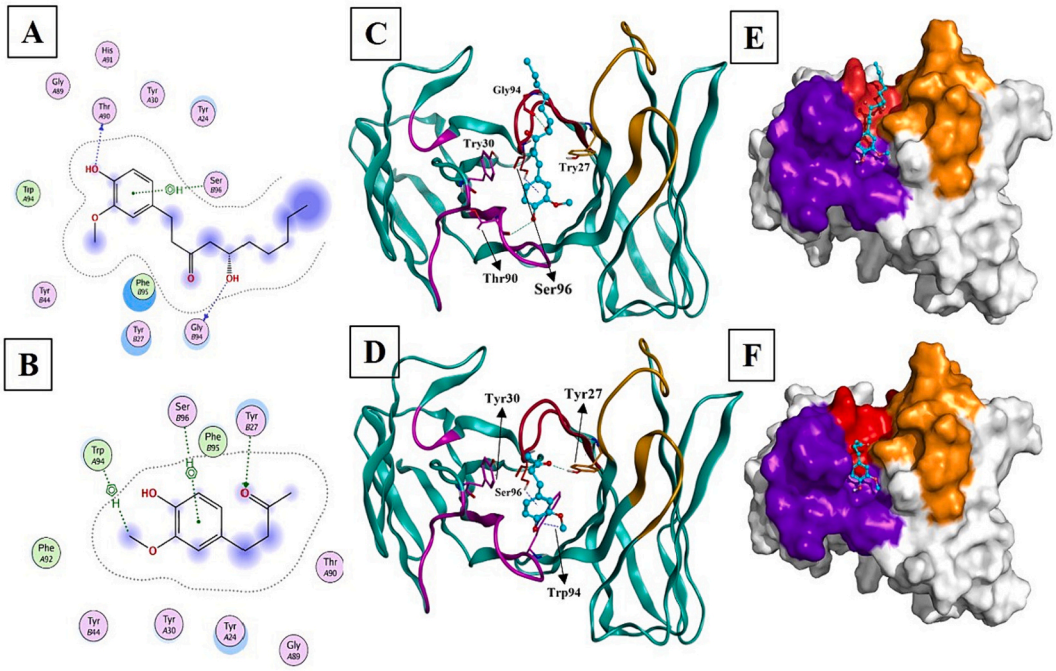

Fig. 1. (A, D)/ (B, E): 2D/3D binding mode depiction of the docked complex of mAbs and 6-GG and VLT, respectively; (C, F): surface morphology of 6-GG and VLT binding with mAbs, respectively.

stirred at 100 °C for 1 h. After stirring at 140 °C for 6 h, the solution was extracted and concentrated. The residue was purified by flash column chromatography using dichloromethane-methanol (TCL: DCM: MeOH = 20:1) as the eluent (obtaining Compound 1–3). 0.3 g was dissolved in 50 mL of methanol, and 0.2 g 10% Pd/C was used for hydrogenation reduction and filtered after stirring for 2 h. After concentrating the remaining samples, they were dissolved in DCM, meanwhile, heated to 40 °C. After recovery to RT, the precipitated white solid was extracted and filtered. The column purified the crude product (TLC: DCM: MeOH: 20:1), the pure Hapten 1 was obtained.

Hapten 7: compound 7–1 (2.28 g, 0.0125 mol) was dissolved in 20 mL TFA, added to urotropine (1.75 g, 0.0125 mol), heated to 75 °C and stirred for 3 h. After removing some TFA, add HCl aqueous solution and extract it two times with trichloromethane, Na_2SO_4 dried, reduced pressure and concentrated. The residue was purified by flash column chromatography using petroleum ether/ethyl acetate (TLC: PE: EA = 2:1) as the eluent, and pure product 7–2 was obtained. Under nitrogen protection, compound 7–2 (0.97 g, 4.6 mmol) was dissolved in 10 ml of methanol, and L-proline (0.66 g, 5.75 mmol) as well as compound 7–3 (0.55 g, 3.85 mmol) was added and stirred for 0.5 h at room temperature. The trifluoroacetic acid (TEA, 1.16 g, 11.5 mmol) was dropped and stirred overnight. The organic layer extracted twice by water and ethyl acetate was dried with Na_2SO_4, concentrated and purified (TLC: PE: EA = 3:1) under reduced pressure to obtain pure product 7–4 about 0.6 g. 0.2 g 10% Pd/C was used for hydrogenation reduction and filtered after stirring for 3 h. After concentrating the remaining samples, they were dissolved in DCM, meanwhile, heated to 40 °C. After recovery to RT, the precipitated white solid was extracted and filtered. The column purified the crude product (TLC: PE: EA = 5:1). 0.22 g of the pure product 7–5 was obtained. Compounds 7–5 (0.2 g, 0.59 mmol) were dissolved in 6 mL THF, and 6 mL of 2 M NaOH solution was added, heated to 80 °C and stirred l h. The organic layer extracted 3 times by water and ethyl acetate was dried with Na_2SO_4, concentrated and purified (TLC: PE: EA = 5:1) under reduced pressure to obtain pure product Hapten 7.

All haptens were coupled with protein (BSA or OVA) by the active ester method through their active carboxylic acid groups. The specific steps were as follows:

First, 20.16 mg of Hapten 1 (25.76 mg of Hapten 7) was dissolved in 0.4 ml DMF, and then added 11.6 mg NHS. After stirring at RT for 30 min, DCC/DMF solution (20.6 mg DCC was dissolved in 0.1 ml DMF) was added dropwise. After stirring at RT for 4 h, the reaction liquid was stood at 4 °C overnight. Then, centrifugation and the supernatant were added dropwise into dissolved BSA/OVA solution (7 mg/ml), and it was stirred for 4 h. The resulting conjugates dialyzed with PBS (pH 7.4) for 60 h at 4 °C. Hapten X-BSA was used as an immunogen, and Hapten X-OVA was a coating antigen.

2.5. Preparation of mAbs

Female Balb/c mice (6–8 weeks) were purchased from the Shandong First Medical University &Shandong Academic of Medical Sciences (Jinan, China) (permit numbers: SCXK 20190003). All animals were handled following Chinese laws and guidelines and were approved by the Medical Ethics Committee of the Shandong University of Technology. The surviving animals in this study were euthanized by cervical dislocation during the study period. Eight female Balb/c mice were divided into two groups performed according to a previous study (Yang et al., 2016) to be immunized with Hapten 1-BSA and Hapten 7-BSA, respectively. Briefly, the antigen in FCA (1:1, *v*/v) emulsified saline was 80 μg, and the antigen was injected subcutaneously in the back at multiple points. After 21 days of immunization interval, 80 μg immunogen was emulsified with FIA (1:1 v/v) for four consecutive times. Mouse antiserum samples were collected starting from the second immunization. The affinity and specificity were detected by indirect noncompetitive ELISA (incELISA) and indirect competitive ELISA (icELISA) (Table S1) (Zhang, Ma, et al., 2022). The analytes concentration in the test were 1 mg/mL, and each analyte was mixed equally.

Two mice with higher titer and sensitivity to CPCs-GDs were selected for cell fusion. Three days before cell fusion, 100 μg antigen was diluted with normal saline to 200 μL and injected intraperitoneally to give impact immunity to mice. Cells were screened using limited dilution subcloning (Bai et al., 2021). After multiple rounds of screening, cells producing highly sensitive bs-mAbs to CPCs-GDs were screened and subjected to mass production using mouse ascites. Bs-mAbs were

purified from ascites using the caprylic acid-ammonium sulfate precipitation method. The bs-mAbs were kept at −20 °C for future use.

2.6. Performance evaluation of mAbs

Purified mAbs were identified by Sodium dodecyl sulfate-polyacrylamide gel electrophoresis (SDS-PAGE).

The titer, sensitivity, and cross-reactivity (CR) of mAbs were evaluated by incELISA and icELISA (Zhang, Ma, et al., 2022). It was homologous ELISA when haptens of immunological antigen and coating antigen in the structure were the same, all the others were heterologous ELISA (Zhang, Ma, et al., 2022). The IC_{50} which were calculated through Origin 2018 software and CR were used to evaluate the sensitivity and specificity of mAbs towards CPCs (CPC, DCPC, N—V), GDs (6-GG, 6-SG, VLT), as well as other eight compounds respectively. The CR was calculated by eq. (1) (Zhang, Zhang, et al., 2022):

$$CR(\%) = [IC_{50}(6-GG)/IC_{50}(test\ compound)] \times 100\% \quad (1)$$

Table 2
Cross-over combinations of mAbs / coated antigens from different sources.

Coating antigens[c]	mAbs	Titer value[a]	IC_{50} (ng/mL)					
			CPC	DCPC	N-V	6-GG	6-SG	VLT
			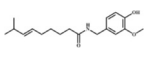	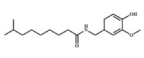	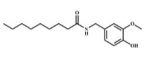	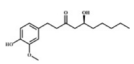	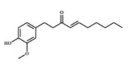	
Hapten 1-OVA	1-F12	1:128000	584.42	557.14	251.58	506.23	974.99	680.32
	1-G12	1:64000	1229.06	700.85	383.16	560.59	1847.86	1020.39
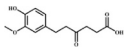	1-D6	1:126000	>4000	969.82	2126.35	59.17	657.56	165.14
	2-LD2	1:1000	118.75	9.47	6.50	24.79	11.72	>4000
	3-LD3	<1000	-[b]	–	–	–	–	–
	4-AT4	1:15000	5.02	5.81	20.14	4.93	25.66	>4000
	5-3H1	1:24000	1159.67	15.98	21.57	38.97	441.24	>4000
	5-D8	1:7000	39.87	5.82	20.61	23.28	223.58	>4000
	6-AT6	1:3000	>4000	>4000	>4000	>4000	>4000	>4000
Hapten 2-OVA	1-F12	1:64000	>4000	>4000	>4000	>4000	>4000	>4000
	1-G12	1:34000	>4000	>4000	>4000	>4000	>4000	>4000
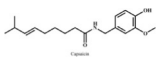	1-D6	1:96000	>4000	>4000	1780.11	1147.33	1897.43	2769.82
	2-LD2	1:32000	9.61	4.85	1.70	1436.16	0.57	>4000
	3-LD3	1:30000	10.16	1.24	1.73	1821.65	6.82	>4000
	4-AT4	1:3000	132.83	57.33	135.50	>4000	>4000	>4000
	5-3H1	1:32000	547	102.63	8.30	>4000	>4000	>4000
	5-D8	1:6000	540.41	166.52	59.50	>4000	>4000	>4000
	6-AT6	1:16000	>4000	>4000	>4000	>4000	>4000	>4000
Hapten 3-OVA	1-F12	1:64000	>4000	>4000	>4000	>4000	>4000	>4000
	1-G12	1:34000	>4000	>4000	>4000	>4000	>4000	>4000
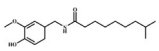	1-D6	1:96000	>4000	>4000	>4000	27.78	1025.79	23.55
	2-LD2	1:40000	17.15	1.54	1.21	1.78	3.26	>4000
	3-LD3	1:32000	30.08	0.62	1.46	2182.32	4.99	>4000
	4-AT4	1:3000	270.36	253.87	41.57	>4000	>4000	>4000
	5-3H1	1:64000	794.17	253.86	242.95	>4000	>4000	>4000
	5-D8	1:8000	564.57	55.75	100.25	>4000	>4000	>4000
	6-AT6	1:16000	>4000	>4000	>4000	>4000	>4000	>4000
Hapten 4-OVA	1-F12	1:128000	796.54	415.85	202.52	401.26	134.01	380.79
	1-G12	1:64000	835.06	724.69	177.53	410.84	136.05	423.72
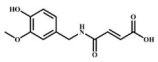	1-D6	1:16000	917.16	701.28	223.85	297.53	133.75	331.25
	2-LD2	1:32000	1.19	0.73	0.03	1.01	2.38	1249.17
	3-LD3	1:16000	3.87	1.84	4.75	271.08	1.37	>4000
	4-AT4	1:8000	6.51	10.68	4.37	>4000	61.38	>4000
	5-3H1	1:64000	25.86	11.35	4.04	1062.82	128.01	>4000
	5-D8	1:8000	28.78	10.90	2.74	1030.07	359.44	>4000
	6-AT6	1:36000	>4000	>4000	>4000	>4000	>4000	>4000
Hapten 5-OVA	1-F12	1:128000	481.51	143.58	88.13	122.83	117.61	283.22
	1-G12	1:64000	339.39	373.58	143.29	195.53	107.14	114.02
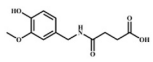	1-D6	1:32000	939.17	588.73	223.33	132.86	71.79	121.68
	2-LD2	<1000	–	–	–	–	–	–
	3-LD3	<1000	–	–	–	–	–	–
	4-AT4	1:4000	3.79	3.13	2.00	481.65	19.64	>4000
	5-3H1	1:48000	103.27	31.24	5.46	670.41	310.76	>4000
	5-D8	1:12000	45.59	13.19	9.81	1036.51	310.76	>4000
	6-AT6	1:15000	>4000	1460.54	637.10	425.62	2926.40	2191.15
Hapten 6-OVA	1-F12	1:4000	1354.43	884.10	438.54	631.69	233.65	219.94
	1-G12	1:4000	661.85	351.51	251.65	284.44	86.21	263.37
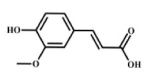	1-D6	1:1000	264.34	167.92	152.52	150.56	50.30	199.80
	2-LD2	<1000	–	–	–	–	–	–
	3-LD3	<1000	–	–	–	–	–	–
	4-AT4	<1000	–	–	–	–	–	–
	5-3H1	<1000	–	–	–	–	–	–
	5-D8	<1000	–	–	–	–	–	–
	6-AT6	1:32000	>4000	>4000	>4000	>4000	>4000	>4000

[a] Titer values was expressed by the dilution ratio of antisera when the OD_{450} value was 1.00 ± 0.20.
[b] The IC_{50} values were not measured because of the low titer value.
[c] The data of Hapten 7-OVA were not given because it failed to induce a significant immune response (Titer value of antiserum were <1000).

2.7. Primary establishment of LFIA

The conjugate of carboxyl-functionalized ZnCdSe/ZnS quantum dots (QDs) (emission maximum at 525 nm) with Goat anti-mouse IgG (QDs-Gm-IgG) and test strips were prepared as mentioned in Yang et al. (Yang et al., 2016).

3. Results and discussion

3.1. Molecular docking-based virtual screening strategy

The purpose of this study was to prepare bs-mAb that can recognize CPCs-GDs to overcome the problems of time-consuming, complicated operation and single detection index in the real-time detection process of gutter cooking oil. The f-groups of small molecules are an essential factor producing of related mAbs. Our previous work has utilized pre-existing 5-D8 for homology modeling (Fig. S2, Fig. S3), and molecular docking with CPCs (Sun et al., 2022). The alignment of FR sequences for the query and the templates were shown in Fig. S2. For the FR, the identities between query and templates were 95.3% and 91.9% for VL and VH, respectively. For the six CDRs, the identities between query and templates are 75%, 100%, 88.9%, 72.7%, 81.3%, and 66.7% for CDR-L1/L2/L3/H1/H2/H3, respectively. To validate the quality of the constructed model, we plotted the Ramachandran plot for the modeled structure, as shown in Fig. S3. All residues were located in the favored or allowed regions, with no outliers observed. In the Verify3D figure, 96.31% of the residues had averaged 3D—1D score $\geq$0.2. This indicated the high quality of this model. On this basis, we performed molecular docking with 6-SG and VLT (Fig. 1, Table S2). Docking simulations were conducted to predict the small molecules' binding mode and binding with 5-D8. The pocket surrounded by the CDRs of 5-D8 was defined as the putative binding site. The binding free energy scores of the 5 molecules were listed in Table S2. The predicted order of binding affinity for the docked compounds to mAbs was DCPC > CPC > N-V > 6-GG > VLT. This showed consistency with the actual test results (Table 2, Hapten 5-OVA/5-D8), which also verified the feasibility of our method.

The key f-groups of the standard structure were analyzed by molecular docking, providing a specific theoretical basis for designing bs-haptens. The binding mode 5-D8 with 6-GG and VLT was illustrated in Fig. 1. 6-GG and VLT have formed a suitable steric complementarity with the binding site of mAbs. Otherwise, a hydrogen bond was formed among 6-GG and VLT with mAbs. The benzene ring group of the ligand formed OH-Pi interaction with the side chain of Ser96 in H-CDR3. VDW interactions were formed among 6-GG and VLT with the surrounding residues. These interactions mainly contributed to the binding energy between 6-GG and VLT with mAbs. In addition, the phenolic hydroxyl oxygen atom and Hydroxyl oxygen atom of 6-GG, regarded as the hydrogen bond donor, formed a hydrogen bond with the oxygen atom in the backbone of Thr90 of L-CDR3 and Gly94 of H-CDR3 in the receptor, respectively. The carbonyl oxygen atom of VLT, regarded as the hydrogen bond acceptor, formed a hydrogen bond with the oxygen atom in the sidechain of Tyr27 of H-CDR1 in the receptor. The ligand formed CH-Pi interaction with the sidechain of Trp94 in L-CDR3.

To more intuitively show the force of different small molecules docking with mAbs, we used the Venn diagram (Table S3 and Fig. S4). By analyzing the docking results of five analytes with 5-D8, we found that the benzene ring, phenolic hydroxyl, methoxy and the carbonyl in long chain alkyl were the main f-groups for the formation of hydrogen bond with 5-D8 (Zou et al., 2022). In other words, these f-groups played an essential role in the immune system, producing the bs-mAbs to CPCs-GDs. Therefore, we used these f-groups as a key factor in designing the hapten of CPCs-GDs. Otherwise, the long-chain alkyl and carbonyl played a clear role in the co-recognition of CPCs-GDs.

3.2. Reverse design of Haptens and computational validation

The objective of the present study was to produce mAbs with high affinity and specificity to CPCs-GDs. With the help of the molecular docking of 5-D8 with 6-GG and VLT, important f-groups such as the benzene ring, phenol hydroxy group, methoxy group, and the carbonyl in long-chain alkyl have been identified. Our previous work found that ESP analysis can effectively improve haptens' screening efficiency, thus significantly reduce the workload in the process of high-quality mAbs preparation (Zhang, Ma, et al., 2022). As shown in Fig. S5, the rigid spacer arm can improve immunogenicity (Xu et al., 2011). In haptens design, link arm sites and the length are also important for the exposure of key f-groups (Spinks, 2000). Based on the above analysis, as shown in Fig. S1, we reverse-designed and synthesized two new haptens, both of which retained the key f-groups mentioned above. The difference was that Hapten 1 introduced the carboxyl group into the long chain end, while Hapten 7 introduced the carboxyl group and decanone on the benzene ring. In addition, CPC, DCPC, and ferulic acid were used as haptens for comprehensive analysis (Wu et al., 2022). The two other reported CPCs haptens were also necessary (Yang et al., 2016).

The steric hindrance and interactions resulting from electronic properties are thought to be primarily responsible for antigen-antibody recognition (Chen et al., 2021). To verify the reliability of the reverse design of haptens, geometric conformation, and ESP analysis were performed (Fig. 2). For haptens which we designed, the electrode area was concentrated in the phenol hydroxy group and the carbonyl in long chain alkyl as well as ester group. Hapten 1–5 had a similar geometric conformation and ESP surface distribution, both of them had a negatively charged phenolic hydroxyl group, negatively charged oxygen atoms on the methoxy group, positively charged methyl group, almost electroneutral benzene ring, negatively charged carbonyl and terminal carboxyl group in the side chain. Meanwhile, both the side chain's nitrogen or hydrogen atoms provided a positively electric surface. These regions, which had the spatial distribution of strong positive or negative electrostatic, may be easy to interact to structures with high polarity to stimulate the body to produce high affinity and high sensitivity mAbs. This was consistent with the results of the immunization experiments. For Hapten 7, the carboxyl group and decanone were introduced into the benzene ring. This increased the strong positive electric region near the phenyl ring (the hydrogen atom on the carboxyl group) and the strong negative electric region (the ester group on the carboxyl group). At the same time, the electroneutral surface of the long chain had a higher hydrophobic nature. ESP analysis of haptens further proved the feasibility of strategies, which used molecular docking between existing mAbs and analytes to identify key f-groups.

There is some relationship between the immune effects and the intermolecular force of the complete antigen after protein conjugation (Xu et al., 2011). To explore the effect of connecting arm sites on the immune system, it was necessary to couple Hapten 1 and Hapten 7 with the lysine tripeptide fragment (Asp-Lys-His) of BSA to simulate their spatial conformation and calculate their potential surface distribution (Fig. 2). The ESP of Hap-1-3 T tended to be linear in structure. Coupled proteins at the end of the long-chain alkyl were more conducive to the exposure of essential f-groups, such as benzene ring, phenol hydroxy, methoxy, and carbonyl in the long-chain alkyl. On the contrary, Hap-7-3 T was not conducive due to protein folding and steric hindrance.

3.3. Preparation and identification of Haptens and conjugates

As shown in Fig. S6, the NMR identification map and data of Hapten 1 are: ^{1}H NMR (400 MHz, Chloroform-*d*) δ 6.82 (d, J = 7.9 Hz, 1H), 6.72–6.62 (m, 2H), 5.48 (brs, 1H), 3.87 (s, 3H), 2.89–2.61 (m, 8H). The peak time in the mass spectra was 5.11, and the content was 98.3%. The NMR identification map and data of Hapten 7 are: ^{1}H NMR (400 MHz, DMSO-d_6) δ 7.11 (s, 1H), 6.73 (s, 1H), 3.69 (s, 3H), 2.70–2.60 (m, 4H), 2.39 (t, J = 7.3 Hz, 2H), 1.41–1.46 (m, 2H), 1.21–1.30 (m,8H), 0.85 (t, J

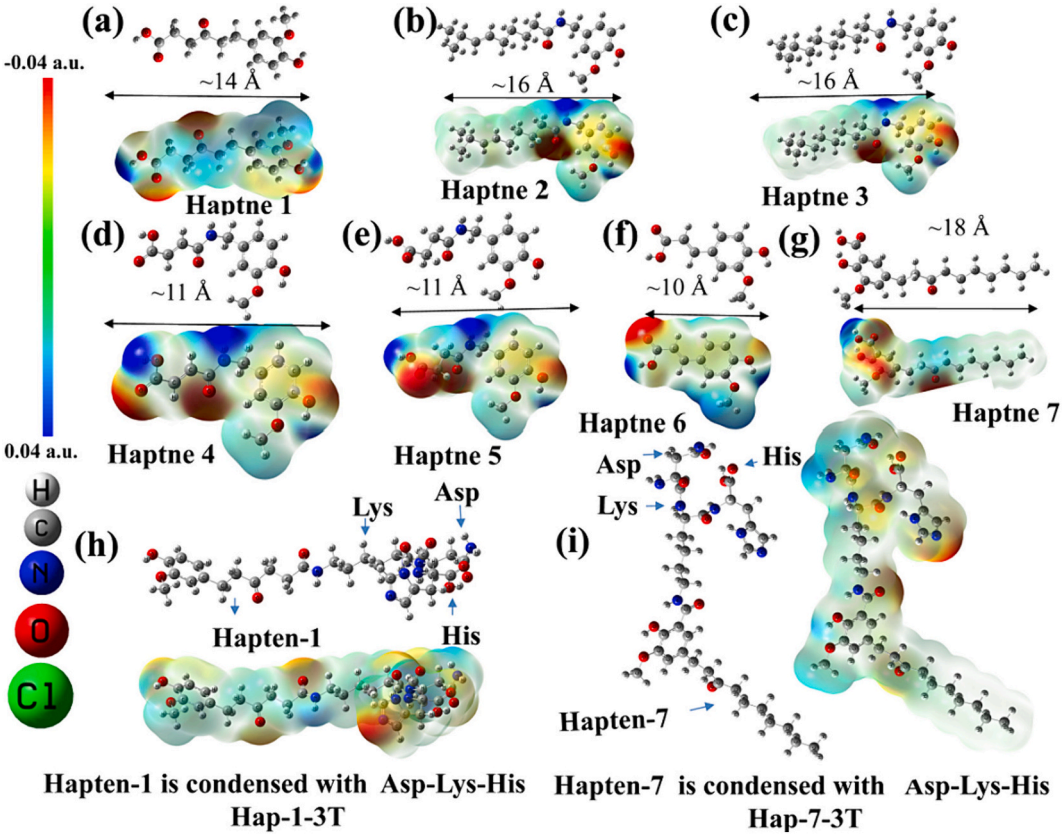

Fig. 2. The optimized structure predicted and its corresponding ESP energy surface at B3LYP/6-311 g (d, p), the equivalent of ESP is set to −0.04 to 0.04 a.u. (a-g) Hapten 1–7; (h-i) the hapten and lysine tripeptide conjugates. (The image of (b-f) reprinted from our previous research (Zhang, Ma, et al., 2022)).

= 6.6 Hz, 3H). The peak time in the mass spectra was 7.53 and the content was 99.3%. The results suggest that the two synthesized hapten compounds are highly pure and suitable for creating complete synthetic antigens. The immunogen and coating antigens were prepared by the active ester method, and they were Hapten X-BSA and Hapten X-OVA, respectively.

3.4. Screening and characterization of antisera and bs-mAbs

Mice immunized with Hapten 1-BSA and Hapten 7-BSA were monitored from secondary immunization (Table S1). By monitoring mouse antiserum, two mice were selected for cell fusion. The detection method was conducted as we reported previously (Zhang, Ma, et al., 2022), including CPCs, 6-GG, and VLT analytes. The failure of Hapten 7-BSA to induce a significant immune response (Best IC_{50} of antiserum >1000 ng/mL) confirmed our hypothesis that steric hindrance between the coupling protein and Hapten 7 led to ineffective exposure of key f-groups. This also reflected that the connecting arm site significantly affected the immune response. The positive cells were subcloned by limiting dilution, and three bs-mAbs to CPCs-GDs were obtained (Fig. S7).

All mAbs were identified by SDS-PAGE, purified mAb with little other protein in the lane, and bs-mAbs were resolved into 25 kDa (light chains) and 70 kDa (heavy chains) by heat-treated. This indicated that mAbs had been successfully prepared and purified (Fig. 3A).

Referring to the icELISA developed in previous work (Zhang, Ma, et al., 2022), we identified the specificity (Table 1), affinity, and sensitivity ((Fig. 3B—D, Table 2) of mAbs under optimal conditions. From Table 2 and Fig. 4, we could know that mAbs prepared using Hapten 1-BSA could meet our real needs in multiple combinations. Both of them had broad spectrum characteristics, and could meet sensitivity requirements in the actual detection. As shown in Table 1, CPCs-GDs and eight other structural analogs were used to assess the specificity of mAbs prepared by Hapten 1-BSA. MAbs had good recognition ability for both CPCs-GDs, while the CR value of other analogs was low. In addition, D4-E6-D6 had a high sensitivity to GDs. Therefore, the subsequent analysis was focused on 1-F12 and 1-G12 (Fig. 3B—D).

In order to overcome the problem of low inhibition rates potentially caused by homologous ELISA, the combination of mAbs from different sources with different coating antigens was necessary. In our study, Hapten 1–5 retained important f-groups, such as the benzene ring, phenol hydroxy group, methoxy group, and the carbonyl in long-chain alkyl. CPC and DCPC were used as Hapten 2 and Hapten 3 (Wu et al., 2022). Meanwhile, Hapten 4 and Hapten 5 have been reported (Yang et al., 2016; Zhang, Ma, et al., 2022). These establish the foundation for heterologous ELISA to improve the sensitivity and specificity of bs-mAbs. In addition, Hapten 6 and Hapten 7 were used to define the effect of carbonyl, connecting arm length and site on the bs-mAbs to CPCs-GDs. At the same time, the high affinity between antibody and analyte can easily lead to low titer and high inhibition rate (Shen et al., 2023). As shown in Table 2 and Fig. 4, six analytes (CPCs-GDs) could be effectively identified by mAbs prepared with Hapten 1-BSA, in multiple combinations. Surprisingly, mAbs prepared with Hapten 2-BSA and Hapten 3-BSA could not effectively recognize VLT in homologous ELISA. Although they showed high sensitivity to five other analytes, the narrow detection range was a defect.

With bs-mAbs as the primary research object, the analysis data shown that bs-mAbs to CPCs-GDs had highest sensitivity when Hapten 5-OVA was coating antigen, followed by Hapten 4-OVA (bs-mAbs to CPCs-GDs had better affinity for Hapten 4-OVA). Combined with the experimental data from these two coating antigens, the titer of the same mAb also confirmed this. This suggested that a carbon–carbon double bond allowed a long-chain alkyl of hapten to form a rigid spacer arm, facilitating the exposure of the key active site in the Hapten 4-OVA. This also

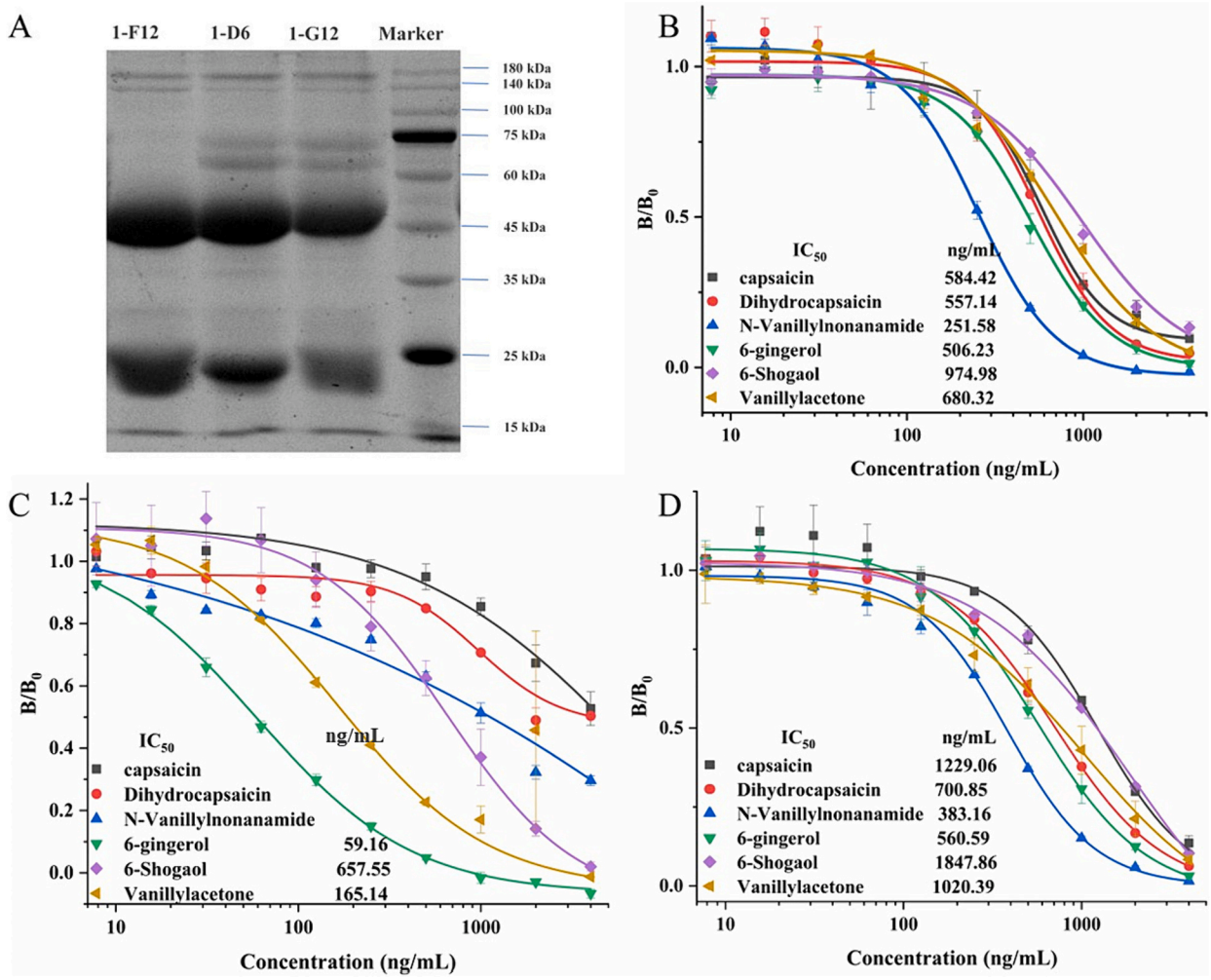

Fig. 3. (A): The reduction results after purification (SDS-PAGE); Sensitivity detection plots of the purified mAbs. (B): 1-F12; (C): 1-D6; (D): 1-G12.

confirmed the conclusions of our previous study (Zhang, Ma, et al., 2022). Interestingly, when Hapten 6-OVA was used as a coating antigen, only mAbs produced by Hapten 1-BSA could effectively recognize all analytes. This suggested that the connecting arm length, long-chain alkyl, and carbonyl played an important role in the immune response. However, when Hapten 2-OVA and Hapten 3-OVA were used as coating antigen, neither Hapten 1-BSA nor Hapten 6-BSA produced mAbs recognized analytes well, which indicated that mAbs produced by Hapten 1-BSA could effectively recognize Hapten 2-OVA and Hapten 3-OVA, with weak recognition to Hapten 6-OVA. At this time, the molecular structures of CPC and DCPC were the same as Hapten 2 and Hapten 3, respectively. It fully indicated that hapten conformation changed, and the active site was exposed after coupling with OVA. MAbs obtained by Hapten 2-OVA and Hapten 3-OVA had poor recognition ability to VLT. It indicated that the amide group was not conducive to producing of bs-mAbs to CPCs-GDs, which was consistent with our prediction. In addition, long chain alkyl played a pivotal role in bs-mAbs production. Due to the diversity of analytes, appropriate modification of long chain alkyl could effectively improve the sensitivity of prepared mAbs for all analytes. The results indicate that Hapten 5-OVA/1-F12 has a high affinity and sensitivity when combining the prepared antigenic antibodies to CPCs and GDs with the collected antigenic antibodies for ELISA (Table 2). As shown in Fig. 5A, the B_0 value was the absorbance value of the reaction solution detected at 450 nm for the incELISA assay without the mixtures of CPCs and GGRs standards solution, the B value was the absorbance value of the reaction solution detected at 450 nm for the icELISA assay with the mixtures of CPCs and GGRs standards solution. The highest sensitivity was observed for N—V with IC_{50} of 88.13 ng/mL and the lowest sensitivity was observed for CPC with IC_{50} of 481.51 ng/mL. Although Hapten 5-OVA/1-F12 has a higher IC_{50} for related analytes, it can detect more species than other studies (Table 3). Therefore, we selected Hapten 5-OVA/1-F12 for the verification of the actual test.

3.5. Development of LFIA

In order to explore the practicability, we conducted the preliminary experiment under the condition of the optimal combination. Mixed analytes of varying concentrations (0, 0.3, 0.4, 0.5, 0.6, 0.7, 0.8, 0.9 and 1 μg/mL) were prepared. The experimental effect was considerable, and the strip showed obvious band change after adding the mixed analytes (Fig. 5B). As the concentration of mixed analytes increased, the T-line color rendering decreased significantly.

4. Conclusions

In this study, we adopted a strategy based on molecular docking to reverse the design and screening of bs-haptens, which innovatively and efficiently defined the key f-groups of the target analytes. The existing CPCs mAbs (5-D8) were used for homology modeling, molecular docking was conducted with CPCs-GDs. Ultimately, the bs-haptens of CPCs-GDs were successfully designed and evaluated. On this basis, ESP analysis and the preparation of bs-mAbs successfully verified the feasibility of our strategy from both theoretical and practical levels. To

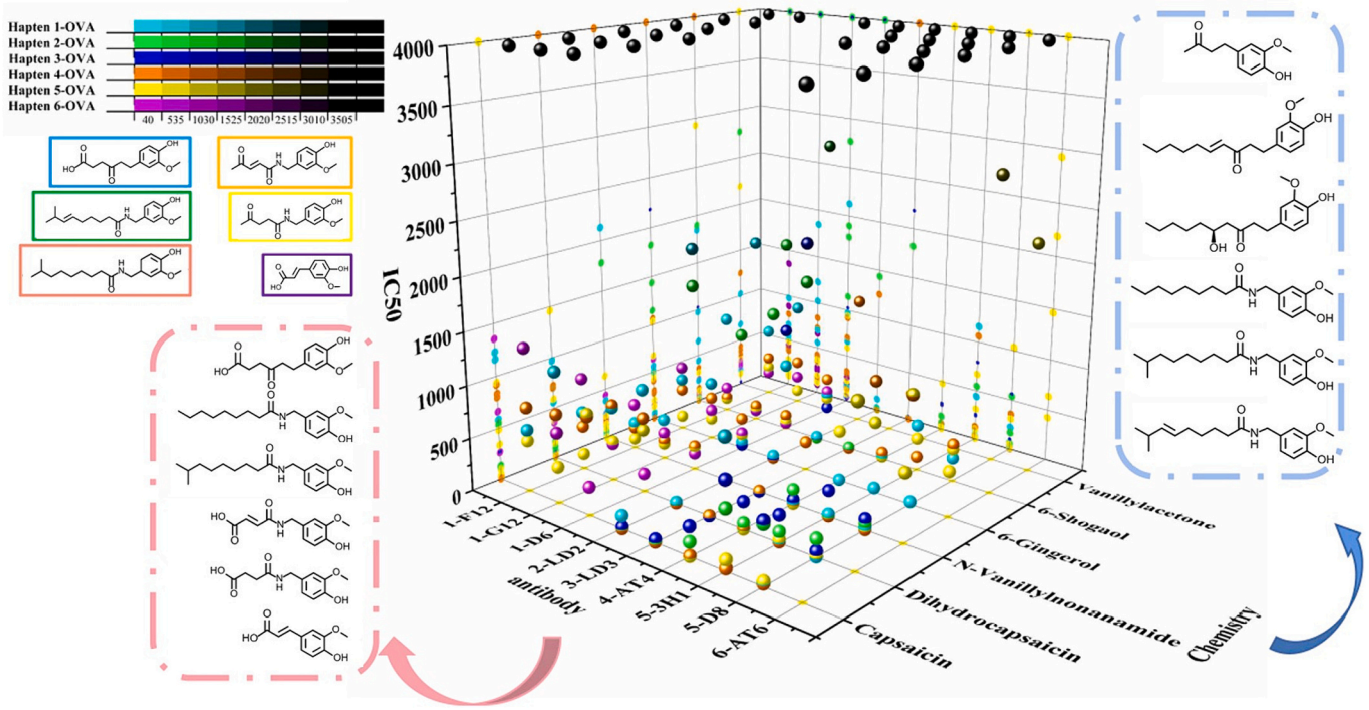

Fig. 4. Scatter plots of the sensitivity comparison of the crossover combinations (The IC_{50} values were shown in 4000 when it was higher than 4000, The IC_{50} values were not measured When the titers were below 1000).

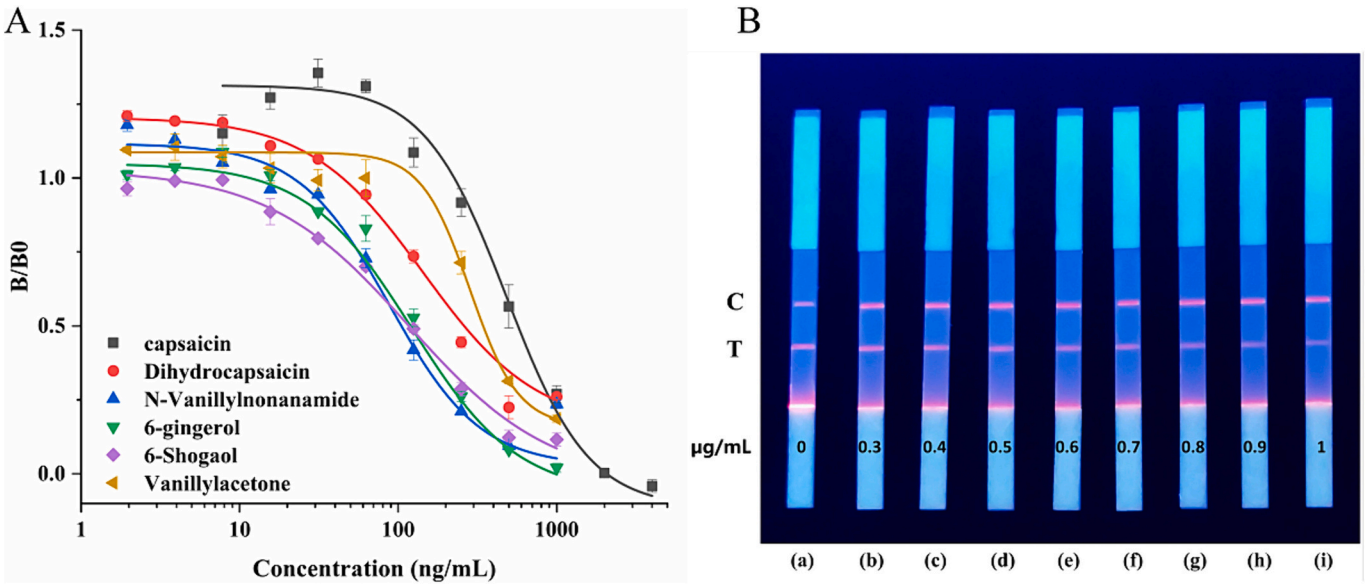

Fig. 5. (A) ELISA inhibition curves for different analytes under the optimal combination (hapten 5-OVA/1-F12); (B) Detection results of LFIA to CPCs-GDs with different concentrations, (a): contrast, (b-i): different concentrations of mixed analytes were added.

further investigate the molecular mechanisms of bs-mAb with antigen recognition, the collection of antigens and mAbs that have been reported was necessary. The results suggested that mAbs derived from the novel hapten showed a more significant advantage and stability. Meanwhile, a rigid spacer arm favored the exposure of the active site, and proper modification of the long-chain alkyl group could effectively improve the sensitivity of preparing bs-mAbs to analytes. Moreover, in the design of broad-spectrum haptens of CPCs-GDs, the amide groups and carbonyl played opposite roles in the immune response, in which the carbonyl was more important. Finally, under the optimal combination (Hapten 5-OVA/1-F12), the IC_{50} to all analytes was intermediate between 88.13 and 499.16 ng/mL. On this basis, the simple development of LFIA was conducted, which verified the possibility of the practical application of bs-mAbs.

Ethical approval

All animal treatments were in strict compliance with Chinese laws and guidelines and conformed to the National Institutes of Health Guide for Care and Use of Laboratory Animals.

Table 3
The monoclonal antibody prepared in this paper was compared with other monoclonal antibodies of capsaicinoids and gingerol derivatives in recent years.

Serial number	Identifiable species of capsaicinoids and gingerol derivatives	IC_{50}[a] (ng/mL)	refes
1	CPC, DCPC, NDCPC, N-V	0.18–0.81	Bai et al., 2021
2	CPC, DCPC, Homodihydrocapsaicin, Nordihydrocapsaicin	0.17–0.27	Wu et al., 2022
3	CPC, DCPC, N-V	47,800–400	Zhang, Ma, et al., 2022
4	CPC, DCPC, N—V, 6-GG, 6-SG, VLT	88.13–499.16	This work

[a] IC_{50} refers to the range of the lowest and highest IC_{50} for the detectable analytes of the antibodies developed in the paper.

CRediT authorship contribution statement

Kunying Nie: Writing – review & editing, Writing – original draft, Visualization, Validation, Software, Investigation, Data curation, Conceptualization. **Jiali Zhang:** Writing – review & editing, Writing – original draft, Visualization, Methodology, Investigation, Formal analysis. **Haitao Xu:** Investigation, Formal analysis. **Keyun Ren:** Validation, Software. **Chunlei Yu:** Validation, Software. **Qi Zhang:** Investigation, Formal analysis. **Falan Li:** Investigation, Formal analysis. **Qingqing Yang:** Supervision, Resources, Methodology, Investigation, Funding acquisition, Formal analysis.

Declaration of competing interest

The authors declare that they have no known competing financial interests or personal relationships that could have appeared to influence the work reported in this paper.

Data availability

No data was used for the research described in the article.

Acknowledgements

This research was supported by the National Natural Science Foundation of China (No. 32161133008, No. 31701681), and was supported by China Postdoctoral Science Foundation (No. 2022M721978).

Appendix A. Supplementary data

Supplementary data to this article can be found online at https://doi.org/10.1016/j.fochx.2024.101273.

References

Abdu-Allah, H. H. M., Wu, S. C., Lin, C. H., & Tseng, Y. Y. (2020). Design, synthesis and molecular docking study of α-triazolylsialosides as non-hydrolyzable and potent CD22 ligands. *European Journal of Medicinal Chemistry, 208*, Article 112707. https://doi.org/10.1016/j.ejmech.2020.112707

Amirav, A., Neumark, B., Margolin Eren, K. J., Fialkov, A. B., & Tal, N. (2021). Cannabis and its cannabinoids analysis by gas chromatography–mass spectrometry with cold EI. *Journal of Mass Spectrometry, 56*(6), Article e4726. https://doi.org/10.1002/jms.4726

Aziz, F., Xin, M., Gao, Y., Chakroborty, A., Khan, I., Monts, J., … Dong, Z. (2020). Induction and prevention of gastric cancer with combined helicobacter pylori and capsaicin administration and DFMO treatment, respectively. *Cancers, 12*(4), 816. https://doi.org/10.3390/cancers12040816

Bai, Y., Jiang, H., Zhang, Y., Dou, L., Liu, M., Yu, W., … Wang, Z. (2021). Hydrophobic moiety of capsaicinoids haptens enhancing antibody performance in immunoassay: Evidence from computational chemistry and molecular recognition. *Journal of Agricultural and Food Chemistry, 69*(34), 9957–9967. https://doi.org/10.1021/acs.jafc.1c03657

Bhattarai, S., Tran, V. H., & Duke, C. C. (2001). The stability of Gingerol and Shogaol in aqueous solutions. *Journal of Pharmaceutical Sciences, 90*(10), 1658–1664. https://doi.org/10.1002/jps.1116

Ceballos-Alcantarilla, E., Abad-Fuentes, A., Agulló, C., Abad-Somovilla, A., & Mercader, J. V. (2021). Immunochemical method for penthiopyrad detection through thermodynamic and kinetic characterization of monoclonal antibodies. *Talanta, 226*, Article 122123. https://doi.org/10.1016/j.talanta.2021.122123

Chapa-Oliver, A. M., & Mejía-Teniente, L. (2016). Capsaicin: From plants to a cancer-suppressing agent. *Molecules, 21*(8), 931. https://doi.org/10.3390/molecules21080931

Chen, Z. J., Wu, H. L., Xiao, Z. L., Fu, H. J., Shen, Y. D., Luo, L., … Xu, Z. L. (2021). Rational hapten design to produce high-quality antibodies against carbamate pesticides and development of immunochromatographic assays for simultaneous pesticide screening. *Journal of Hazardous Materials, 412*, Article 125241. https://doi.org/10.1016/j.jhazmat.2021.125241

Crapnell, R. D., & Banks, C. E. (2021). Electroanalytical overview: The pungency of Chile and chilli products determined via the sensing of capsaicinoids. *Analyst, 146*(9), 2769–2783. https://doi.org/10.1039/d1an00086a

Dalsasso, R. R., Valencia, G. A., & Monteiro, A. R. (2022). Impact of drying and extractions processes on the recovery of gingerols and shogaols, the main bioactive compounds of ginger. *Food Research International, 154*, Article 111043. https://doi.org/10.1016/j.foodres.2022.111043

Guo, Z., Li, X., Gao, F., Zhang, Q., & Li, H. (2016). Determination of capsaicinoids in edible oil by liquid chromatography-isotope dilution mass spectrometry. *Chemical Reagents, 38*(6), 491–495. https://doi.org/10.13822/j.cnki.hxsj.2016.06.001

Huang, Z. M., Xin, J. X., Sun, S. S., Li, Y., Wei, D. X., Zhu, J., … Yao, Y. F. (2021). Rapid identification of adulteration in edible vegetable oils based on low-field nuclear magnetic resonance relaxation fingerprints. *Foods, 10*(12). https://doi.org/10.3390/foods10123068

Javaheri-Ghezeldizaj, F., Mahmoudpour, M., Yekta, R., & Dolatabadi, J. E. N. (2020). Albumin binding study to sodium lactate food additive using spectroscopic and molecular docking approaches. *Journal of Molecular Liquids, 310*, Article 113259. https://doi.org/10.1016/j.molliq.2020.113259

Li, L., Hou, R., Shen, W., Chen, Y., Wu, S., Wang, Y., … Peng, D. (2021). Development of a monoclonal-based ic-ELISA for the determination of kitasamycin in animal tissues and simulation studying its molecular recognition mechanism. *Food Chemistry, 363*, Article 129465. https://doi.org/10.1016/J.foodchem.2021.129465

Lu, F., & Wu, X. (2014). China food safety hits the "gutter". *Food Control, 41*, 134–138. https://doi.org/10.1016/j.foodcont.2014.01.019

Ma, F., Yang, Q., Matthäus, B., Li, P., Zhang, Q., & Zhang, L. (2016). Simultaneous determination of capsaicin and dihydrocapsaicin for vegetable oil adulteration by immunoaffinity chromatography cleanup coupled with LC–MS/MS. *Journal of Chromatography B, 1021*, 137–144. https://doi.org/10.1016/j.jchromb.2015.12.017

Najar-Ahmadi, S., Haghaei, H., Farajnia, S., Yekta, R., Dolatabadi, J. E. N., & Rashidi, M. R. (2021). Interaction of donepezil with tau protein: Insights from surface plasmon resonance and molecular modeling methods. *Journal of Molecular Liquids, 333*, Article 115924. https://doi.org/10.1016/j.molliq.2021.115924

Promdam, N., Khuituan, P., & Panichayupakaranant, P. (2022). Effects of standardized [6]-gingerol extracts and [6]-gingerol on isolated ileum and lower esophageal sphincter contractions in mice. *Food Chemistry, 378*, Article 132077. https://doi.org/10.1016/j.foodchem.2022.132077

Rifna, E. J., Pandiselvam, R., Kothakota, A., Rao, K. S., Dwivedi, M., Kumar, M., … Ramesh, S. V. (2022). Advanced process analytical tools for identification of adulterants in edible oils–a review. *Food Chemistry, 369*, Article 130898. https://doi.org/10.1016/j.foodchem.2021.130898

Shen, J., Shan, J., Zhu, X., Yang, P., Zhang, D., Liang, B., … Dai, Z. (2020). Sex specific effects of capsaicin on longevity regulation. *Experimental Gerontology, 130*, Article 110788. https://doi.org/10.1016/j.exger.2019.110788

Shen, R., Guan, T., Li, Z., Hong, Z., Dzantiev, B. B., Zherdev, A. V., … Lei, H. (2023). Identifying an emergent adulterant hydrochlorothiazide in food: A simple lateral flow strip with high sensitivity by time-resolved fluorescence. *Food Control, 143*, Article 109265. https://doi.org/10.1016/j.foodcont.2022.109265

Spinks, C. A. (2000). Broad-specificity immunoassay of low molecular weight food contaminants: New paths to utopia! *Trends in Food Science & Technology, 11*(6), 210–217. https://doi.org/10.1016/S0924-2244(01)00009-7

Sun, X., Zhao, Q., Zha, C., Zhang, J., Zhou, Z., Dong, H., … Zhao, S. (2022). Competitive electrochemical immunosensor for detection of capsaicinoids in edible vegetable oil based on computer aided molecular modeling. *Journal of the Electrochemical Society, 169*(5), Article 057502. https://doi.org/10.1149/1945-7111/ac690c

Tan, J., Li, R., Jiang, Z. T., Tang, S. H., Wang, Y., Shi, M., … Wang, H. (2017). Synchronous front-face fluorescence spectroscopy for authentication of the adulteration of edible vegetable oil with refined used frying oil. *Food Chemistry, 217*, 274–280. https://doi.org/10.1016/j.foodchem.2016.08.053

Visciano, P., & Schirone, M. (2021). Food frauds: Global incidents and misleading situations. *Trends in Food Science & Technology, 114*, 424–442. https://doi.org/10.1016/j.tifs.2021.06.010

Wang, M., Gao, B., Xing, Y., & Xiong, X. (2020). Preparation of an electrochemical sensor based on multi-walled carbon nanotubes/molecularly imprinted polymers for the detection of capsaicin in gutter oil by differential pulse voltammetry. *International Journal of Electrochemical Science, 15*(9), 8437–8449. https://doi.org/10.20964/2020.09.09

Wang, T., Wu, H. L., Long, W. J., Hu, Y., Cheng, L., Chen, A. Q., & Yu, R. Q. (2019). Rapid identification and quantification of cheaper vegetable oil adulteration in camellia oil by using excitation-emission matrix fluorescence spectroscopy combined with chemometrics. *Food Chemistry, 293*, 348–357. https://doi.org/10.1016/j.foodchem.2019.04.109

Wu, Q., Yao, L., Qin, P., Xu, J., Sun, X., Yao, B., … Chen, W. (2021). Time-resolved fluorescent lateral flow strip for easy and rapid quality control of edible oil. *Food Chemistry, 357*, Article 129739. https://doi.org/10.1016/j.foodchem.2021.129739

Wu, Y., Liu, J., Yu, J., Zhuang, J., Ma, F., Tan, J., & Shen, Z. (2022). A monoclonal antibody for identifying capsaicin congeners in illegal cooking oil and its applications. *Talanta, 250*, Article 123686. https://doi.org/10.1016/j.talanta.2022.12368

Xu, L., Xu, X., Xiong, H., Chen, L., & Li, Y. (2014). Rapid detection of vegetable cooking oils adulterated with inedible used oil using fluorescence quenching method with aqueous CTAB-coated quantum dots. *Sensors and Actuators B: Chemical, 203*, 697–704. https://doi.org/10.1016/j.snb.2014.07.008

Xu, Z. L., Wang, H., Shen, Y. D., Nichkova, M., Lei, H. T., Beier, R. C., … Sun, Y. M. (2011). Conformational changes of hapten-protein conjugates resulting in improved broad-specificity and sensitivity of an ELISA for organophosphorus pesticides. *Analyst, 136*(12), 2512–2520. https://doi.org/10.1039/c1an15053g

Xu, Z. L., Xie, G. M., Li, Y. X., Wang, B. F., Beier, R. C., Lei, H. T., … Sun, Y. M. (2009). Production and characterization of a broad-specificity polyclonal antibody for O, O-diethyl organophosphorus pesticides and a quantitative structure–activity relationship study of antibody recognition. *Analytica Chimica Acta, 647*(1), 90–96. https://doi.org/10.1016/j.aca.2009.05.025

Yang, H., He, Q., Eremin, S. A., Pan, J., Zou, Y., Cui, X., & Zhao, S. (2021). Fluorescence polarization immunoassay for rapid determination of dehydroepiandrosterone in human urine. *Analytical and Bioanalytical Chemistry, 413*(17), 4459–4469. https://doi.org/10.1007/s00216-021-03403-7

Yang, Q., Zhu, J., Ma, F., Li, P., Zhang, L., Zhang, W., … Zhang, Q. (2016). Quantitative determination of major capsaicinoids in serum by ELISA and time-resolved fluorescent immunoassay based on monoclonal antibodies. *Biosensors and Bioelectronics, 81*, 229–235. https://doi.org/10.1016/j.bios.2016.02.074

Yang, Z., Zhou, Q., Wu, W., Zhang, D., Mo, L., Liu, J., & Yang, X. (2022). Food fraud vulnerability assessment in the edible vegetable oil supply chain: A perspective of Chinese enterprises. *Food Control, 138*, Article 109005. https://doi.org/10.1016/j.foodcont.2022.109005

Ye, Q., & Meng, X. (2022). Highly efficient authentication of edible oils by FTIR spectroscopy coupled with chemometrics. *Food Chemistry, 385*, Article 132661. https://doi.org/10.1016/j.foodchem.2022.132661

Zeng, L., Guo, L., Wang, Z., Xu, X., Song, S., Xu, L., … Xu, C. (2021). Immunoassays for the rapid detection of pantothenic acid in pharmaceutical and food products. *Food Chemistry, 348*, Article 129114. https://doi.org/10.1016/j.foodchem.2021.129114

Zhang, J., Ma, F., Zha, C., Yang, Q., Zhang, Q., Zhang, W., … Sun, X. (2022). Effect of hapten structures on development of novel antibody against capsaicin and dihydrocapsaicin. *Chinese Journal of Analytical Chemistry, 50*(9), Article 100134. https://doi.org/10.1016/j.cjac.2022.100134

Zhang, J., Zhang, M., Yang, Q., Wei, L., Yuan, B., Pang, C., … Guo, Y. (2022). A simple and rapid homogeneous fluorescence polarization immunoassay for rapid identification of gutter cooking oil by detecting capsaicinoids. *Analytical and Bioanalytical Chemistry, 414*(20), 6127–6137. https://doi.org/10.1007/s00216-022-04177-2

Zou, R., Guo, Y., Chen, Y., Zhao, Y., Zhao, L., Zhu, G., … Guo, Y. (2022). Computer-aided profiling of a unique broad-specific antibody and its application to an ultrasensitive fluoroimmunoassay for five N-methyl carbamate pesticides. *Journal of Hazardous Materials, 426*, Article 127845. https://doi.org/10.1016/j.jhazmat.2021.127845